Scanning-Beam Antenna on Metamaterials Coplanar Structure for Wireless Applications

Abdelaziz Hamdi, Abdelaziz Samet
UR-CSE Research Group
Polytechnique School of Tunisia
Tunisia
abdelaziz.hamdi@polymtl.ca

Journal of Digital Information Management

ABSTRACT: *A scanning-beam antenna on metamaterial coplanar structures is presented. The proposed antenna is, in essence, a composite of Right/Left-Handed (CRLH) coplanar waveguide (CPW) structure incorporating distributed periodic structures with L-C high-pass filter topology which support left-handed (LH) waves. The negative refractive index (NRI) properties of these structures are shown theoretically, numerically and validated by full-wave simulations. The supported LH wave is fully characterized and based on the composite right/left-handed transmission-line (CRLH-TL) theory; and the dispersion characteristics, refractive indexes and Bloch impedance are derived theoretically. In addition, formulas to extract equivalent-circuit parameters from full-wave simulation are given. Since the distance d between adjacent cells of the array is small, $d << \lambda_o$ and the array becomes a uniform leaky-wave antenna (LWA) for a 10-cell operating near 10 GHz. Simulated radiation pattern, gain, and associated loss budget are presented. The results of LWA exhibit scanning-beam capability from backfire-to-endfire direction and accord well with the theoretical analysis. The antenna is printed on thin and flexible substrate ($h = 25\ \mu m$). Furthermore, since the antenna is implemented with low-cost and CPW technology, it is a good candidate for integrated RF/microwave systems that can be used in digital wireless communications and radars.*

Categories and Subject Descriptors
C.2.1 [Network Architecture and Design Wireless communication] **B.1.4 [Microprogram Design Aids] B.7 [Integrated circuits**] Gate arrays

General Terms: Metamaterials, Wireless Applications, Antenna unit cell

Keywords: Scanning-Beam Antenna, Coplanar Structure, Microwave systems

Received: 4 January 2011, Revised 19 February 2011, Accepted 24 February 2011

1. Introduction

Over the past decade, Electromagnetic metamaterials have become an extremely active field of research in both wireless systems and engineering communities [1-6]. Since Oliner [7] first reported the leaky-wave structure, many microstrip LWA designs incorporating various modifications have been explored. Recently, Eleftheriads [8, 9], Caloz. [10, 11] have proposed a metamaterial-based backward radiating LWA on microstrip transmission line (TL).

This paper offers a fresh perspective on the operation of LH media that enables the modeling and the design of a scanning-beam antenna on CPW structure with negative refractive index. The main of this choice is explained by the advantages offered by CPW [12] over conventional microstrip line are: First, it reduces radiation loss; second, it facilitates easy shunt as well as series surface mounting of active and passive devices; third, it eliminates the need for wraparound and via holes, and fourth, it simplifies fabrication.

The proposed LWA is capable of continuously scanning the beam and contains 10-cell improved performance, such as wider scanning, high gain, and small unit cell (UC) size, and it offers several distinct advantages at X-band frequencies. The antenna is realized using flexible substrate material with dielectric constant $\varepsilon_r = 3.4$ and thickness $h = 25\ \mu m$. The thin dielectric provides embedded planar capacitance capability, which represents one of the constituent elements of the CLRH antenna unit cell.

In addition, beamwidth can be changed, in general, by a phased array of antennas or by geometrical parameters [13, 14]. In this work, we present a new concept in which beamwidth is adjustable in a frequency change while keeping geometrical parameters unchanged and using a single antenna.

The obtained results show an improved type of a backfire-to-endfire LWA on coplanar structure. At low frequency ($f_L = 9$ GHz, $f_L < f_o$), this structure is LH (propagation constant $\beta < 0$) and therefore radiates backward. At high frequency ($f_R = 12$ GHz, $f_R > f_o$), it is RH ($\beta > 0$) and radiates forward. At the transition frequency ($F_o = 10$ GHz, $\beta = 0$), it radiates broadside.

2. Circuit model of antenna unit cell

2.1 Approximation principle

In reality, a purely LH-Cell is unrealizable because the effect of the discrete periodic loading (L_R-C_R) of the host transmission-line medium (RH) cannot be neglected. Therefore, the topology of Figure 1(a) represents the most general form of a CRLH UC model to design a metamaterials structures with LH attributes, as shown in Figure 1(b). Practically, the length Δd is less then $\lambda_g/5$ and the resulting structure is a *high-pass* filter mimicking the LH-TL in its pass-band.

We consider here only the lossless case, which can be straightforwardly extended to lossy case [15]; we consider also the balanced case that is defined by $L_R C_L = L_L C_R$ with the advantage of providing a more direct insight into the physical characteristics of the line.

The proposed artificial CLRH TL can be virtually realized in any technology. However, it can be artificially released in the form of a lumped-element distributed network. The CRLH TL is ideal in the sense that it transmits energy from dc to ∞, and does not exist in nature, particularly because of its LH range. One possibility consists in periodically repeating an electrically small lumped unit cell, shown in Fig. 1, into an artificial line.

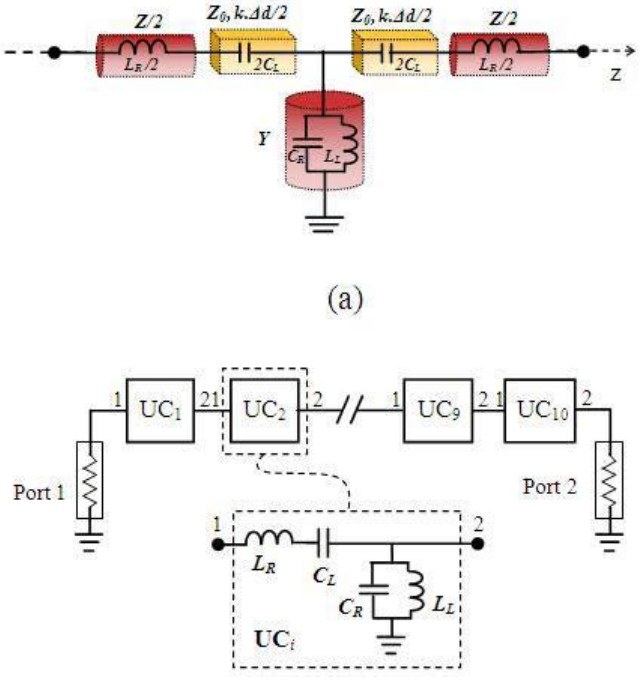

Figure 1. Circuit model. (a) UC for 1-D periodic distributed CRLH TL with host media (Z_0, k, d), (b) CRLH TL for the 1-D periodic L–C network with 10 cells. The parameters L_R, C_R, L_L and C_L are expressed in *[H/m], [F/m], [H.m]* and *[F.m]* respectively

The behavior of the artificial CRLH-UC of Fig. 1(a) is a bandpass filter with a stopband from dc to the LH cutoff frequency

$$f_{c,L} = \frac{1}{4\pi\sqrt{L_L C_L}} \quad (1)$$

and a stopband from the RH cutoff frequency to ∞ ($f_{C,L} < f_{C,R}$)

$$f_{c,R} = \frac{1}{\pi\sqrt{L_R C_R}} \quad (2)$$

The proposed antenna is designed for a transition frequency equal to 10 GHz and the input/output characteristic impedance of the CPW is fixed to 100 Ω for $N = 10$ cell. Using these data, and the balanced case condition, we can easily extract the four circuit parameters (L_R, C_R, L_L, C_L). The RHM and LHM unit cell inductor and capacitor are judiciously specified as (L_R = 1 nH, C_R = 0.1 pF) and (L_L = 2.5 nH et C_L = 0.25 pF) respectively. Furthermore, the cutoff-frequencies $f_{C,L}$ and $f_{C,R}$ are found to be 3.18 GHz and 31.83 GHz respectively.

Finally, the designed RHM and LHM network with lumped elements are appropriately terminated with matching resistors on all edges and simulated with the ADS microwave circuit simulator.

The desired dispersion relation of this circuit model can be obtained through standard periodic analysis based upon the 1-D symmetric unit cell in Fig. 1(a) where its expression is given by

$$\cos(\beta d) = \cos(\theta) + \frac{ZY}{2}cos^2\left(\frac{\theta}{2}\right) + \frac{j}{2}\left(\frac{Z}{Z_0} + \frac{Y}{Y_0}\right)\sin(\theta) \quad (3)$$

where $\theta = kd$ and d is the period of the unit cell. In general, the effect of the discrete distributed elements of the host transmission-line medium cannot be neglected. In the full dispersion relation given by (3), it is clear that β can become periodically complex, choosing the circuit parameters as aforementioned, the dispersion diagram of (3), for a balanced case ($L_R C_L = L_C L_R$, represented by solid line) and unbalanced case [15] ($L_R C_L \neq L_C L_R$, dashed line) LC-based, is depicted in Fig. 2.

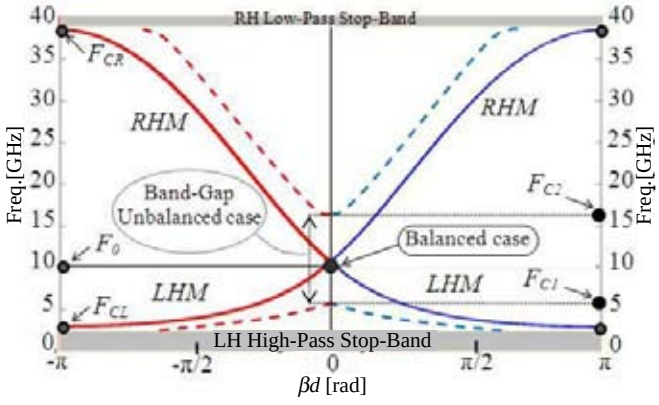

Figure 2. Dispersion diagram for a balanced (solid) and unbalanced (dashed) 1-D CRLH TL

As shown, the LHM and RHM can be identified and the pass-bands are observed, separated by a finite stopband (indicated by the band-gap in the unbalanced case). The lowest cutoff frequency (Bragg) associated with this dispersion curve (indicated in Fig. 2 by f_{CL}) is approximately determined by (1) to be equal to 3.18 GHz. The CRLH circuit exhibits two eigen-frequencies that are expressed as follows:

$$f_{c1} = \frac{1}{2\pi\sqrt{L_R C_L}} \text{ and } f_{c2} = \frac{1}{2\pi\sqrt{L_L C_R}} \quad (4)$$

In this work, having the matching mode (balanced case), both frequencies in (4) are equal to 10 GHz and correspond to the resonant frequencies of the series resonant branch (L_R, C_L) and parallel antiresonant branch (L_L, C_R), respectively. Based on this mode, these braches cross at a unique point on the axis ($\beta=0$). This point corresponds to transition frequency (f_0), equals 10 GHz. Whereas, if these frequencies are different, (or unbalanced case), a band-gap appears between the LH and RH branches, limited by f_{c1} and f_{c2} as shown in dispersion diagram of Fig. 2.

2.2 Results for Antenna cells using lumped elements

The simulation results for LC-based CRLH TL, using the extracted parameters (L_R = 1 nH, C_R = 0.1 pF, L_L = 2.5 nH and C_L = 0.25 pF) in a ten-cell coplanar waveguide CRLH TL are shown in fig. 3. The *S*-parameters results for different number of unit-cells (N = 1, 3, 10) are depicted in Fig. 3(a,b). Consequently, according to the return loss (S_{11}) and insertion loss (S_{21}), the cutoff frequency f_c of the resulting high-pass filter decreases when N increases. Excellent agreement can be observed, which shows that the circuit model with extract parameters (*at* $f_c = f_0 = 10$ *GHz*) is accurate and can be potentially used in the more complicated problem of the antenna, which will be described in the following sections. Fig. 3(b) and equation (1) provide an exact approximation of cutoff frequency for $N > 3$. It can be seen that if the bandwidth is to be increased (toward lower frequencies), larger values of capacitance and inductance

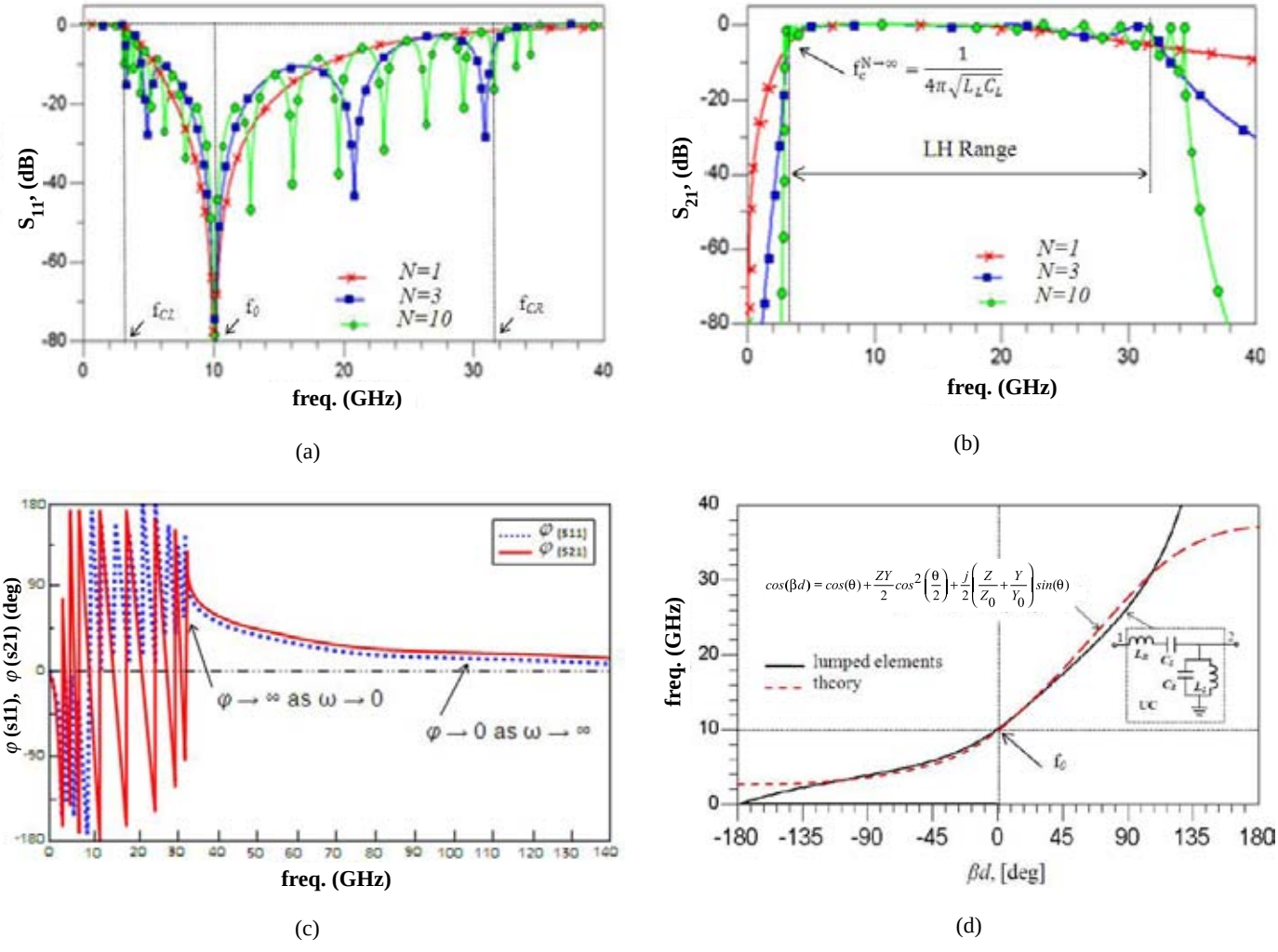

Figure 3. Simulation results for antenna UC with the ideal lumped-element shown in Figure 1 (balanced case). (a) Magnitude of the S_{11} versus N = 1; 3; 10. (b) Magnitude of the S_{21} versus N = 1; 3; 10. (c) Phase of the S-parameters for N = 10, where the sign of $\varphi\{S_{11}\}$ changes at f_0 = 10 GHz. (d) βd-ω diagram, computed from $\varphi\{S_{21}\}$ for lumped-elements unit cell, compared to theoretical results shown in Figure 2.

are required due to the larger number of unit-cells to keep the characteristics of the CRLH transmission line unchanged.

An apparent paradox of the LHM is related to the frequency dependence of its guided wavelength. Whereas, in a RH-TL, $\lambda_{g,RHM}(\omega) = 2\pi/(\omega\sqrt{L_R C_R}) \propto 1/\omega$, the guided wavelength in the LHM is

$$\lambda_{g.LHM}(\omega) = \frac{2\pi}{|\beta_L|} = 2\pi\omega\sqrt{L_L C_L} \propto \omega \qquad (5)$$

The frequency dependence (1) of λ_g is clearly seen in the distribution of peaks of S_{11}, which become more and more distant when ω increases, the highest frequency peak corresponding to an electrical length of the line of $d_{el} = \lambda_g/4$. Fig. 3(c) shows the phase of the S-parameters in the ideal CRLH transmission line. The phase $\varphi\{S_{21}\} = 0$ as $\omega \to \infty$ (at open circuit), and it progressively accumulates as frequency decreases so that eventually at $\varphi\{S_{21}\} = \infty$ as $\omega \to 0$, as it can be revealed by unwrapping the phase curve. Finally, Fig. 3(d) demonstrates the dispersion diagram obtained by the unwrapped phase of S_{21} as follows:

$$\beta d = -\varphi\{S_{21}\} \qquad (6)$$

The dispersion curves of the ideal LH unit cell with lumped elements can also be seen to be in excellent agreement with the theoretical curve (3) of the fictitious line (Fig.3), specifically at the transition frequency f_0 = 10 GHz.

3. Antenna Implementation Using Cpw

3.1 Antenna unit cell design

In general, distributed-element implementations, with nondispersive L/C components, will naturally provide the best results. Any physical implementation of these structures at RF/microwave frequencies must be a periodic one and must, therefore, possess a certain infinitesimal size. However, the needed dimensionality perturbs slightly the homogeneity of the distributed system. In this work, we consider a practical planar design that periodically loads a host CPW network with discrete reactive elements. Every CPW unit cell (CPW-UC) can generate the required inductances (L_R and L_L) and capacitances (C_R and C_L). The motivation of this choice is twofold: first, coplanar waveguide does not need via-hole; second, a distributed structure such as a CPW topology will potentially provide better performances at high frequencies. The proposed CPW LH unit cell of antenna consists of a capacitor obtained using a gap on the CPW center conductor and symmetrical *shorted-stub* meander inductances as shown in Fig. 4. The component capacitance/inductance used is strongly dispersive, which will necessarily introduce some discrepancy with respect to the ideal case.

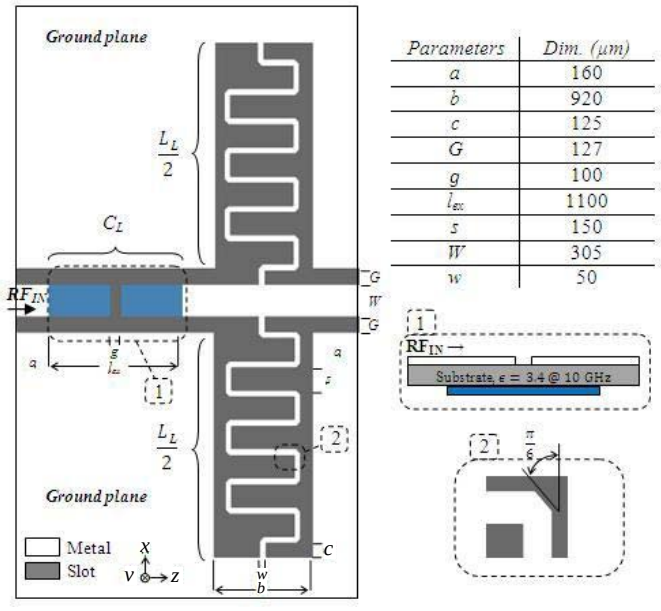

Figure 4. UC prototype of the CPW implementation of the CRLH-TL, including a series capacitor (C_L=0.25 pF) on the center conductor and symmetrical stub meander inductors ($2L_L$ // $2L_L$ = 2.5nH) with their dimensions at 10 GHz

3.2 Antenna unit cell results

The dimensions of the unit cell are given to fabricate the designed antenna at 10 GHz, on 25 μm substrate of ε_r = 3.4. The commercial method of moments software ADS (Advanced Design System) has been used in designing the prototype of the UC. To obtain the characteristically desired values of the LHM (L_L = 2.5 nH and C_L = 0.25 pF), gaps in the CPW center conductor (feed line, RF_{IN}) with bottom metal plaques are served as series capacitors; and to keep the symmetry of the coplanar structure, two short meander inductors are used as shown in Fig. 4.

The antenna unit cell is optimized, at the transition frequency f_0 = 10 GHz, to provide low insertion loss (S21 < 5 dB) which is still reasonable in comparison with the huge losses (S_{21} < 30 dB) reported in [16]. Fig. 5(a) and 5(b) show UC-performances, obtained by full-wave simulation, such as return loss and insertion loss. Very good agreement can be observed with the L-C circuit model, from dc to 20 GHz. This agreement has been also verified for phase where $\varphi(S_{11}, S_{21})$ changes the sign at f_0 = 10 GHz, as shown in Fig. 5(b).

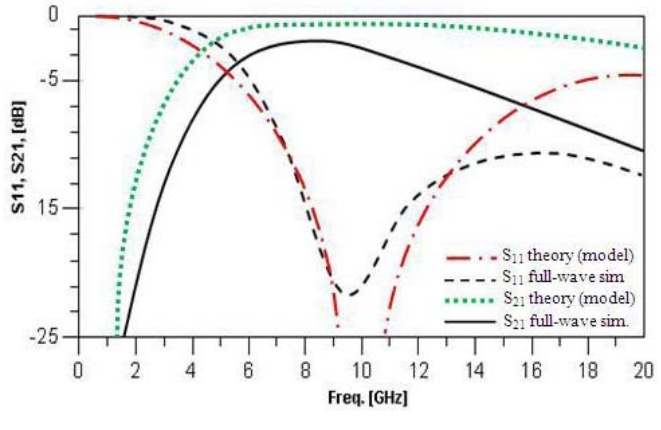

(a)

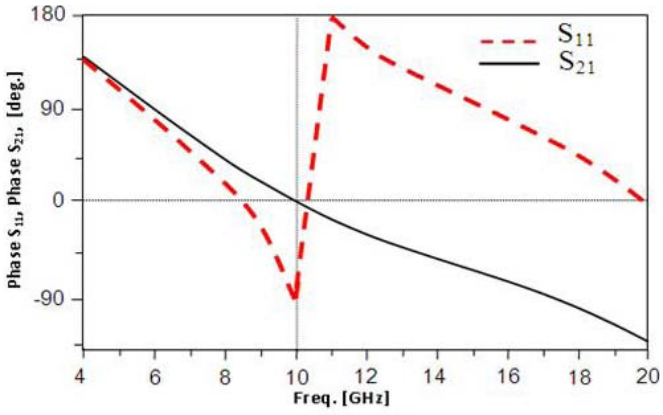

(b)

Figure 5. Full-wave simulation of the unit cell shown in fig. 4, (a) Magnitude of $S_{11}$and S_{21}, (b) Phase S_{11} and S_{21}

Fig. 6 shows the dispersion curve obtained by full-wave simulation with the extracted circuit parameters (L_R = 1 nH, C_R = 0.1 pF, L_L = 2.5 nH and C_L = 0.25 pF). Depending on the operating frequency, the CRLH leaky-wave antenna exhibits left-handed or right-handed behavior.

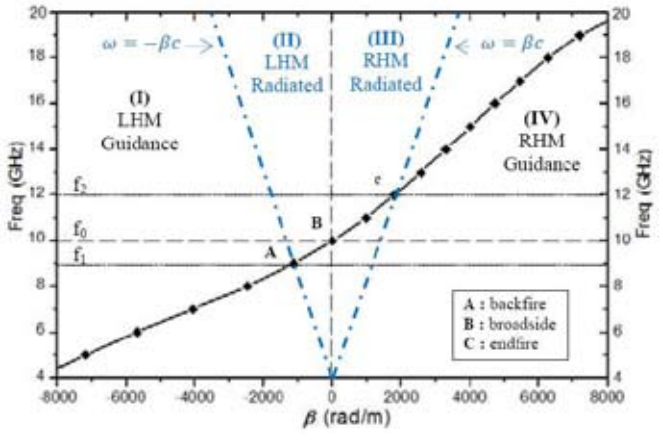

Figure 6. Dispersion diagram of the structures of fig. 4, obtained by full-wave simulation

At low frequencies, the structure operates in the LH mode ($\beta < 0$) and the wave propagates backward since the phase velocity ($v_p = \omega/\beta$) and the group velocity ($v_g = d\omega/d\beta$) are antiparallel. At high frequencies, the structure operates in the RH mode ($\beta > 0$) and the wave propagates forward since v_p and v_g are parallel. At the transition frequency ($\beta = 0$), the structure radiates in the broadside direction thanks to nonzero group velocity. This dispersion diagram is seen to be very close to the theoretical curve (Fig. 3(d)) in the LH range, despite some slope discrepancy, expected from the dispersion of the series capacitors and shunt inductors.

3.3 Antenna implementation and results

A 10-UC of Fig. 4 is used to realize the desired antenna as shown in Fig. 7. A realizable antenna structure would, however, include small CPW-length between adjacent series capacitors and shunt inductors. The proposed antenna is designed using flexible substrate material, Kapton-E[1] polyimide film with dielectric constant ε_r = 3.4 at the operating frequency f_o = 10 GHz (loss tangent = 0.004) and thickness h = 25 μm. The thin

[1]Kapton-E is a registered trademark of El Dupont de Nemours and Company.

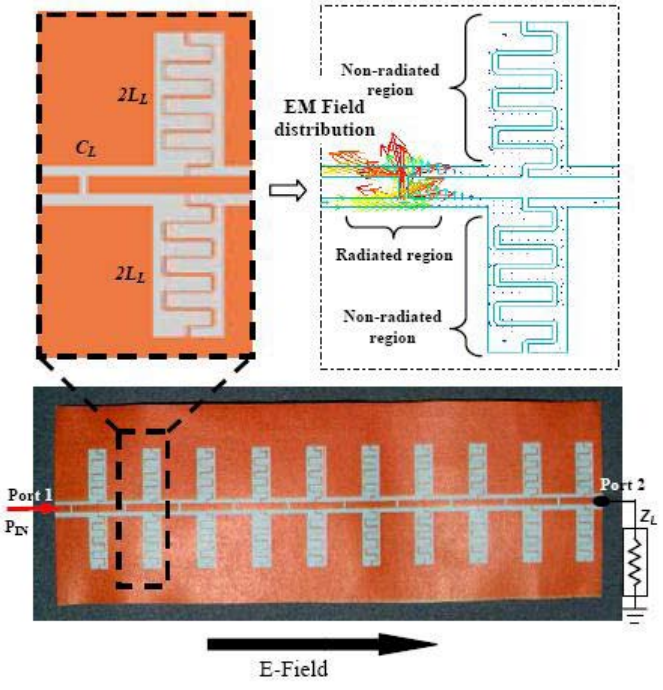

Figure 7. Prototype view of the proposed scanning-beam antenna with electromagnetic field distribution along each cell. The E-field polarization is along the z-direction

dielectric provides embedded planar capacitance capability, which represents one of the constituent elements of the CLRH metamaterials antenna unit cells. The LH capacitance/ inductance are C_L = 0.25 pF and L_L = 2.5 nH, which yields the cutoff frequency f_{CL} = 3.18 GHz. The length of the unit cell is 2.7 mm. the unit cell repeated periodically and the length of the entire antenna is around 27 mm.

The electromagnetic field, over each unit cell of the antenna, has been explored by ADS simulator. It is in fact the capacitive gaps that radiate in this structure while the inductive meander lines are non-radiating due to the anti-parallel currents flowing on each pair of inductive meander lines. This odd symmetry causes cancellation in the far-field and to low cross-polarization levels.

It is demonstrated that CRLH structure is applicable to a frequency-dependent backfire-to-endfire leaky-wave antenna. Fig. 8 shows

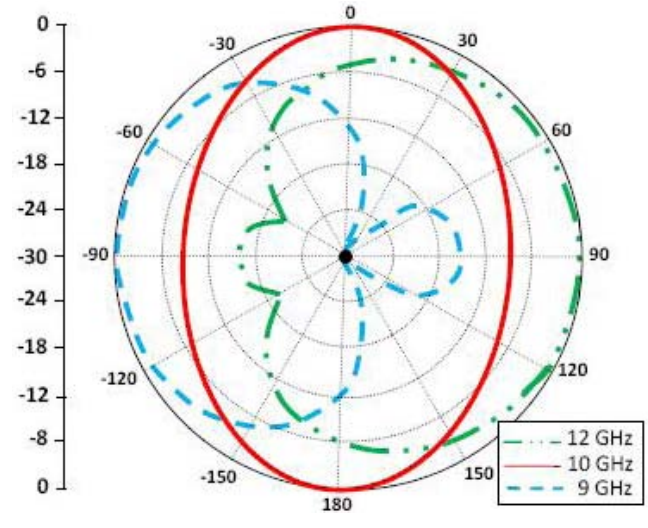

Figure 8. Radiation patterns of the backfire-to-endfire CRLH LWA at 9 GHz, 10 GHz, and 12 GHz

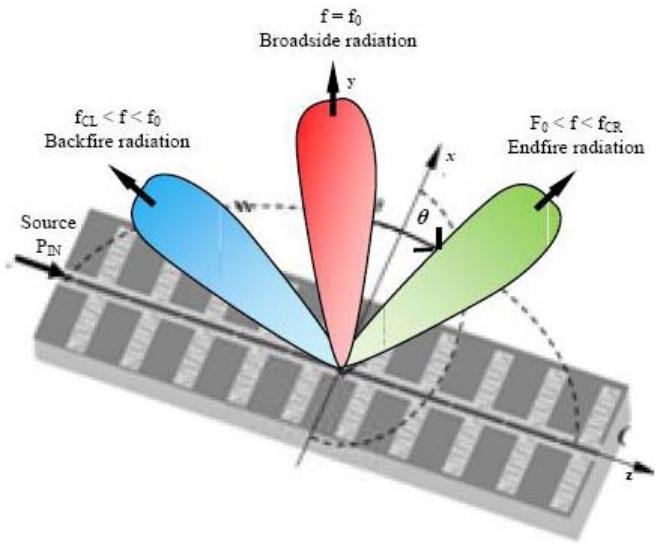

Figure 9. A backfire-to-endfire scanning-beam operation, where f_{CL}, f_0, and f_{CR} are equal to 9 GHZ, 10 GHZ, and 12 GHz, respectively

the measured radiation pattern of the proposed antenna. The obtained results show an improved type of a backfire-to-endfire LWA on coplanar structure.

At low frequency (f_{CL} = 9 GHz, f_{CL} < f < f_o), this structure is LH (β < 0) and therefore radiates backward. At high frequency (f_{CR} = 12 GHz, f_o < f < f_{CR}), it is RH (β > 0) and radiates forward. At the transition frequency (f_o = 10 GHz, β = 0), it radiates broadside as virtually depicted in Fig. 9. Excellent agreement can be observed between measurement and theoretical predictions based on dispersion diagram approach. Finally, a flow design of proposed structure is shown in Fig. 10. These processes can be generalized to design other microwave devices using CRLH metamaterials.

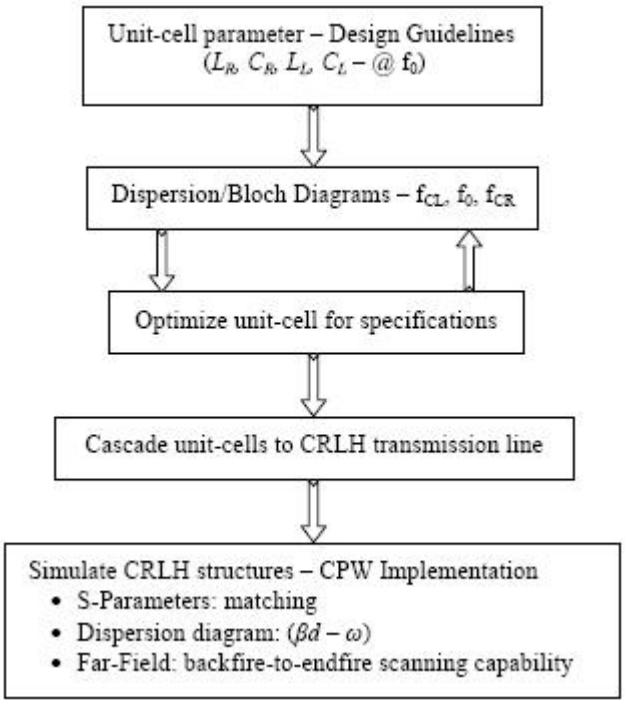

Figure 10. Flow design of the proposed antenna

4. Conclusion

A technique has been demonstrated for implementing novel electronically-controlled scanning-beam antenna on metamaterial coplanar structures. A CRLH transmission-line model has been introduced and discussed in detail to understand the operation of the new scanning-beam antenna and facilitate its design. Based on this model and refinements through method of moments electromagnetic simulations, the proposed CRLH leaky-wave antenna has been characterized and designed at 10 GHz, with CPW configuration on a thin and flexible substrate which exhibits all functions and performances superior to the prior state of the art. The equations to extract the equivalent-circuit parameters L_R, C_R, L_L, C_L, and cutoff-frequencies from the dispersion characteristics and Bloch impedance have been successively provided and validated by full-wave simulation. It has been confirmed that with ideal components, left-handedness can be achieved without losses over an unlimited bandwidth, starting from the cutoff of the resulting high-pass filter and extending to infinity. It has also been shown that an excellent agreement with the theoretical ω-β diagram is obtained. The characterization of the antenna unit cell has been carried out based on the CRLH-circuit theory which has been successfully obtained by full-wave simulation with a good level of accuracy.

Finally, the entire antenna implementation, which supports backward-wave using series capacitors and short stub-inductors without needing the via-holes, has been clearly investigated. It has been demonstrated that the capacitive gaps represent the radiated elements while the inductive meander lines are non-radiating due to the anti-parallel currents flowing on each pair of inductive meander lines. A scanning-beam from backfire-to-endfire direction has been successfully obtained. At low frequency (f_L = 9 GHz, $f_L < f_o$), the antenna radiates backfire. Therefore, this antenna may be applicable to digital wireless broadband systems requiring efficient channelization, such as World Interoperability for Microwave Access (WiMax, IEEE 802.16). Furthermore, since the antenna is implemented with low-cost and CPW technology, it is a good candidate for integrated millimeter-wave systems due to low-cost and its easy fabrication.

References

[1] Wong, A., Eleftheriades, G. V (2010). Adaptation of Schellkunoff's superdirective antenna theory for the realization of superoscillatory antenna arrays, *IEEE Antennas and Wireless Propagation Letters*, 9, p. 315-318.

[2] Engheta, N., Ziolkowski, R.W (2006). Electromagnetic Metamaterials: Physics and Engineering Explorations, *Wiley-IEEE Press*.

[3] Markos, P., Soukoulis, C.M (2008). Wave Propagation: From Electrons to Photonic Crystals and Left-Handed Materials, Princeton University Press.

[4] Eleftheriades, G.V. (2009). EM transmission-line metamaterials, *Materials Today*, 12, p. 30-41.

[5] Monti, G., Tarricone, L. (2005). A Novel Theoretical Formulation for the Analysis of the Propagation of Finite-bandwidth Signals in a Double-negative Slab, *Microwave Optical Technology Letters*, 47, p. 434-439.

[6] Marqués, R., Martín, F., Sorolla, M (2008). Metamaterials with Negative Parameters: Theory, Design and Microwave Applications, Wiley Interscience.

[7] Oliner, A., Lee, K (1986). Microstrip leaky wave strip antennas, *In*: Proc. IEEE Int. Antennas Propagat. Symp. Dig., Philadelphia, PA, p.443-446.

[8] Grbic, A., Eleftheriades, G.V. (2002). A backward-wave antenna based on negative refractive index L-C networks, *In*: IEEE International Symposium on Antennas and Propagation, San Antonio, TX, 4, p. 340-343, June 16-21.

[9] Selvanayagam, M., Eleftheriades, G.V (2010). A compact printed antenna with an embedded double-tuned metamaterial matching network, *IEEE Trans. on Antennas and Propagat*., 58 (7) 2354-2361.

[10] Lim, S., Caloz, C., Itoh, T. (2004). A reflecto-directive system using a composite right/left-handed (CRLH) leaky-wave antenna and heterodyne mixing, *IEEE Microwave Wireless Compon. Lett*., 14 (4,) 183-185.

[11] Nguyen, H. V., Parsa, A., Caloz, C (2010).Power-recycling feedback system for maximization of leaky-wave antennas radiation efficiency, *IEEE Trans. Microwave Theory Tech*., vol. 58, no. 7, pp. 1641-1650, July 2010.

[12] Simons, R. N. (2001). Coplanar Waveguide Circuits, Components, and Systems, John Wiley and Sons, pp. 22-27, 2001.

[13] James, J., Evans, G., Fray, A(1993). Beam scanning microstrip arrays using diodes, Proc*. Inst. Elect. Eng. Microwaves, Antennas, Propagat*., 140, p. 43-51, Feb.

[14] Korisch, I. A., Rulf, B (2000). Antenna beamwidth control using parasitic subarrays, *In*: IEEE AP-S Int. Symp. Dig., p. 117-120, Nov.

[15] Caloz, C., Itoh, T (2005). Electromagnetic Metamaterials: Transmission Line Theory and Microwave Applications, Wiley, New York.

[16] Smith, D. R., Padilla, W. J., Vier, D. C. Nemat-Nassser, S. C., Schultz, S (2000). Composite medium with simultaneously negative permeability and permittivity, *Phys. Rev. Lett*., 84 (18) 4184–4187.